S1. Bonfire/firework locations during bonfire night 2014.

Locations of nine parks with main bonfire/fireworks during November 5th 2014.

Figure S1: Manchester map with locations of parks with bonfires/fireworks displays (red flames) and monitoring site (blue dot) at the University of Manchester. Map produced with Google Maps and location of bonfires was taken from [http://www.pocketmanchester.com/bonfire-night-2014-in-manchester/, accessed 03/05/2017].

S2. Back trajectories for the different pollutant episodes.

Hysplit model was used to run back trajectories, with 48 hrs of duration and three different hights (0, 205 and 500 m about ground level), for the episodes with different pollutant concentrations: a period with high secondary pollutants is observed from October 30th – November 1st; a period with low concentrations from November 1st – 3rd. Bonfire night from November 5th – 7th; a period with high primary emissions from November 8th -10th.

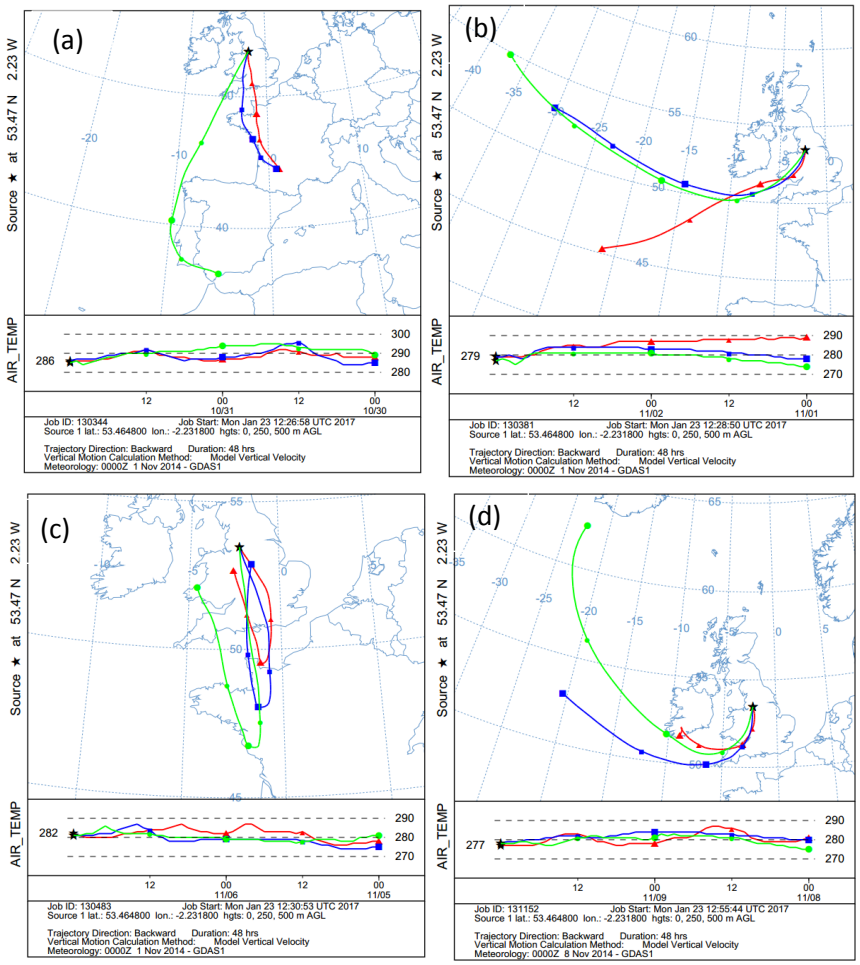

Figure S2: Back trajectories run for events with high secondary pollutant concentrations (a), low pollutant concentrations (b), bonfire night (c) and winter-like event (d).

S3. Aethalometer correction.

Aethalometer measurements (absorption coefficients, b_{ATN}) need to be corrected from two main effects: filter loading (R) and scattering correction (C) that compensates for the multiple-scattering effects from the matrix. There are different methods to correct aethalometer data (Weingartner et al., 2003;Arnott et al., 2005;Schmid et al., 2006). Coen et al. (2010) proposed a new method through a critical analysis of the effectiveness of the other methods, which involves corrections based on absorption and scattering measurements. In this study, wavelength-dependent scattering measurements were not available (A Photo Acoustic Soot Spectrometer was used to measure aerosol optical absorption coefficients. However, the scattering channels failed to report data during the bonfire event), thus the Weingartner method (Weingartner et al., 2003) was used to do these corrections.

The light attenuation (ATN) is defined by equation S1, where I_o is the intensity of the incoming light and I is the remaining light after passing through the filter.

$$\mathrm{ATN} = -100 * \ln\left(\frac{I_o}{I}\right) \quad \text{(S1)}$$

The attenuation cross section (σ_{ATN} in $m^2.g^{-1}$) is calculated using the equation S2, where 14625 [$m^2.g^{-1}$] is the mass specific attenuation cross-section proposed by the manufacturer and λ is the wavelength in nm.

$$\sigma_{\mathrm{ATN}\_\lambda} = \frac{14625}{\lambda} \quad \text{(S2)}$$

The absorption coefficient (b_{ATN}, Mm^{-1}) was calculated using equation S3, where BC is black carbon [$\mu g.m^{-3}$] measured by the aethalometer.

$$b_{ATN\_\lambda} = BC_\lambda * \sigma_{ATN\_\lambda} \quad \text{(S3)}$$

$b_{\_ATN\_\lambda}$ values need to be corrected by calculating b_{abs} (corrected absorption coefficient).

$$b_{abs\_\lambda} = \frac{b_{ATN\_\lambda}}{C*R} \quad \text{(S4)}$$

Where C is a parameter for scattering correction and R, a wavelength dependent parameter, is related to the filter loading effect.

C is calculated as the slope of b_{ATN_630} from aethalometer and b_{abs_630} from MAAP, using the values with ATN<10% (Calculating C with this approach the effects from filter loading are minimized). The Aethalometer does not measure at 630 wavelength thus $b_{ATN\_630,}$ is calculated using equation S6, where the absorption Ångström exponent (α) is calculated using equation S5.

$$\alpha = \frac{\ln\left(\frac{b_{ATN_{470}}}{b_{ATN_{950}}}\right)}{\ln\left(\frac{950}{470}\right)} \quad \text{(S5)}$$

$$b_{ATN\_630} = b_{ATN\_660} * \left(\frac{630}{660}\right)^{-\alpha} \quad \text{(S6)}$$

C represents the slope of b_{ATN_630} from aethalometer vs b_{abs_630} from MAAP. Following this method, a value of C = 3.16 was calculated.

The shadowing parameter (f) is determined, similar to other studies (Sandradewi et al., 2008;Sciare et al., 2011;Ji et al., 2017) as the average of b_{ATN} ratios after and before filter changes for the complete dataset in order to minimise the difference before and after filter changes. The f values obtained were f_{470} = 1.49 and f_{950} = 1.28.

R is calculated with the following equation:

$$R = \left(\frac{1}{f} - 1\right)\frac{ln(\text{ATN}) - ln(10\%)}{ln(50\%) - ln(10\%)} + 1 \quad \text{(S7)}$$

Finally, with C and R being determined, the corrected absorption coefficients (b_{abs_λ}) are calculated with equation S4.

S4. Aethalometer model.

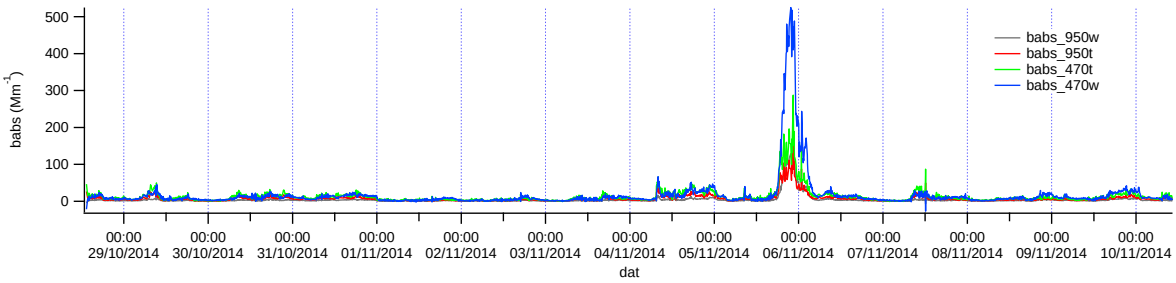

Figure S3: Absorption coefficients (b_{abs}) for wood burning and traffic.

S5. Paticulate organic nitrate (PON) estimation using 46:30 ratios.

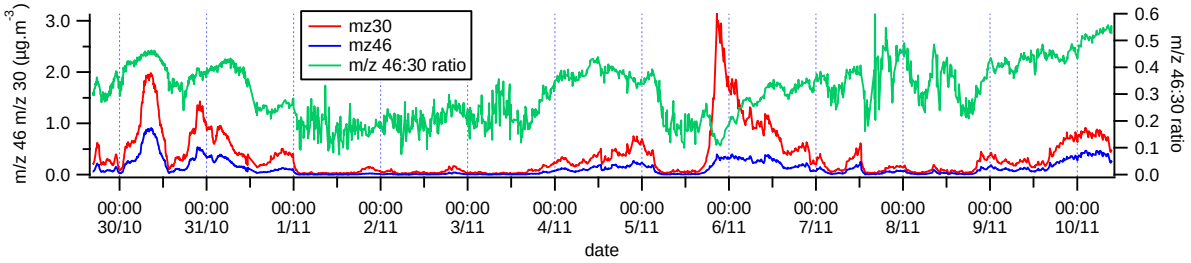

Figure S4: Time series of m/z 46:30 ratio.

Concentrations of PON were calculated following the method proposed by Farmer et al. (2010) and the considerations used by Kiendler-Scharr et al. (2016).

$$X_{PON} = \frac{(R_{meas} - R_{Cal})(1+R_{ON})}{(R_{ON} - R_{cal})(1+R_{meas})} \quad \text{(S8)}$$

R_{cal} = 0.5 is obtained from NH_4NO_3 calibrations, R_{meas} is the measured ambient m/z 46:30 ratios. Following Kostenidou et al. (2015) consideration, R_{ON} = 0.1 as the minimum 46:30 ratio observed was 0.1. The lowest value observed during bonfire night was 0.1.

$$PON = X_{PON} * NO_3^- \quad \text{(S9)}$$

NO_3^- is the total nitrate measured by the AMS.

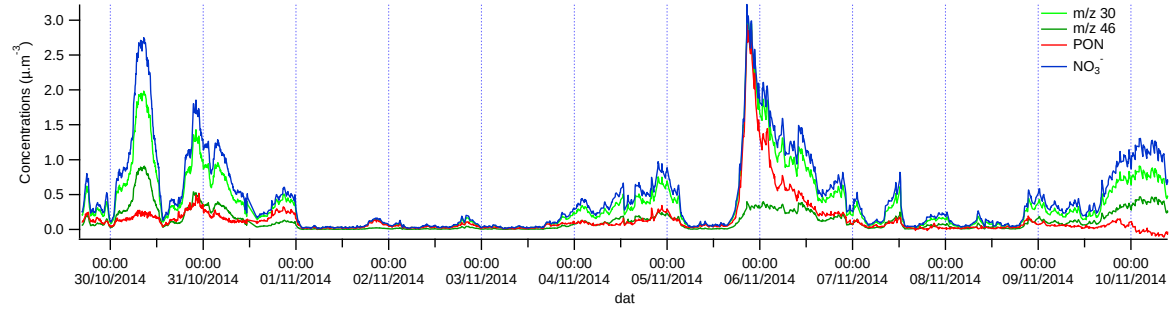

Figure S5: PON concentrations during the whole measurement period.

S6. OA source apportionment.

PMF and ME-2 source apportionment analysis was performed following the strategy proposed by (Reyes-Villegas et al., 2016). A series of solutions were run under different conditions in order to determine the best way to deconvolve OA factors. PMF was run with f-peaks from -1.0 to 1.0 and steps of 0.1. ME-2 was run using different a-values to partially constrain the solutions (table S1), using mass spectra (BBOA, HOA and COA) from Young et al. (2015a) and Crippa et al. (2013) as target profiles (TP). Figure S6 shows the labelling used to identify the different runs performed with ME-2 and table S1 shows the different a-value combinations used to explore different solutions.

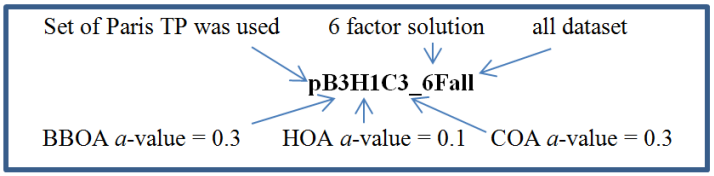

Figure S6: Labelling used to identify runs.

TableS1: List of ME-2 runs

Run	Run
B5H2C5	H1C3
B3H1C3	H2C5
B3H1C5	B3H1
B5H1C5	B5H2
B5H1C3	

Table S2 shows the chosen solutions from the different tests performed.

S6.1 Strategy to select the solution that best apportions OA sources.

The OA source apportionment was performed using different f-peaks when running PMF and different a-values when running ME-2 (table S1) looking at solutions with 4, 5 and 6 factors,. These solutions were explored comparing their residuals and Q/Qexp for m/z's and time series; Total Q/Qexp and total residuals; diurnal profiles and trilinear regression (Reyes-Villegas et al., 2016). Trilinear regression is performed between BBOA, HOA and COA and NOx, since these three OA sources and NOx are related to combustion sources. The chi square value is used as goodness of fit, thus the lowest the value the best correlation between the different sources

Here the analysis carried out to all the dataset is explained in detail.

Step 1. PMF runs looking at 4-factor solutions with f-peaks from -1.0 to 1.0 and steps of 0.1. One solution is chosen to be compared with ME-2 solutions.

Step 2. ME-2 runs looking at 4-factor solutions with different a-values using TP from Paris and London.

Step 3. Two solutions from step 2 are chosen together with the PMF solution, form step 1, to be the three 4-factor solutions to use in the further comparison.

Step 4. Repeat steps 1 to 3 to look at 5-factor and six-factor solutions to finally compare the 9 solutions.

Step 5. Choose one solution that better separates, according to this analysis, OA sources. Perform this analysis for the four tests mentioned in table S2 in order to have one solution for each test.

These steps were used to explore solutions for the different tests performed, generating more than 60 different plots that were analysed. Here, in order to avoid making an overly massive supplement material, only the final comparison between solutions from the different tests performed is shown (Section S6.2). Table S2 shows the chosen solution for each one of the tests performed.

S6.2 Chosen solutions for the different tests.

Table S2: Tests done to determine the solution that better deconvolves OA factors.

Analysis			Solution		Strategy
ID	a	b	a	b	From solution a to b
Test 1	° all		pH1C3_5all		
Test 2	* nbf	bfo	pB3H1C3_5nbf	× nB3H1C5_6bfo	nbf mass spectra were used as TP to analyse bfo dataset.
Test 3	+ bfo	all	PMF_6_0.7	Δ bB5H2C5_5all	bfo mass spectra were used as TP to analyse all dataset.
Test 4	nbf	all	pB3H1C3_5nbf	× nH2C5_5all	nbf mass spectra were used as TP to analyse all dataset.
Test 1_ON	° all		wB3H1_ON_5all		

Test 2_ON	* nbf	bfo	pH1C3_ON_5nbf	nB5H1C3_ON_6bfo	nbf mass spectra were used as TP to analyse bfo dataset.

° all = the whole dataset was analysed: 29/Oct/2014-10/Nov/2014
* nbf = not bonfire period: from 29/Oct to 05/Nov 15:00 and from 06/Nov 06:35 to 10/Nov/2014
+ bfo = bonfire only period: 05/Nov 15:00 - 06/Nov 06:35
× n = mass spectra from analysis a (nbf) were used as TP in the analysis b.
Δ b = means mass spectra from analysis a (bfo) were used as TP in the analysis b for test 3.
ON means the tests performed after modifying the fragmentation table in order to determine an organic nitrate source.

When doing two analyses with ME-2 (in the case of tests 2, 3 and 4), in analysis "a" mass spectra from London (Young et al., 2015b), labelled as "w" and Paris (Crippa et al., 2013) labelled as "p" , were used as target profiles (TP). PMF runs were explored with different fpeak values ranging from -1.0 to 1.0 with steps of 0.1.

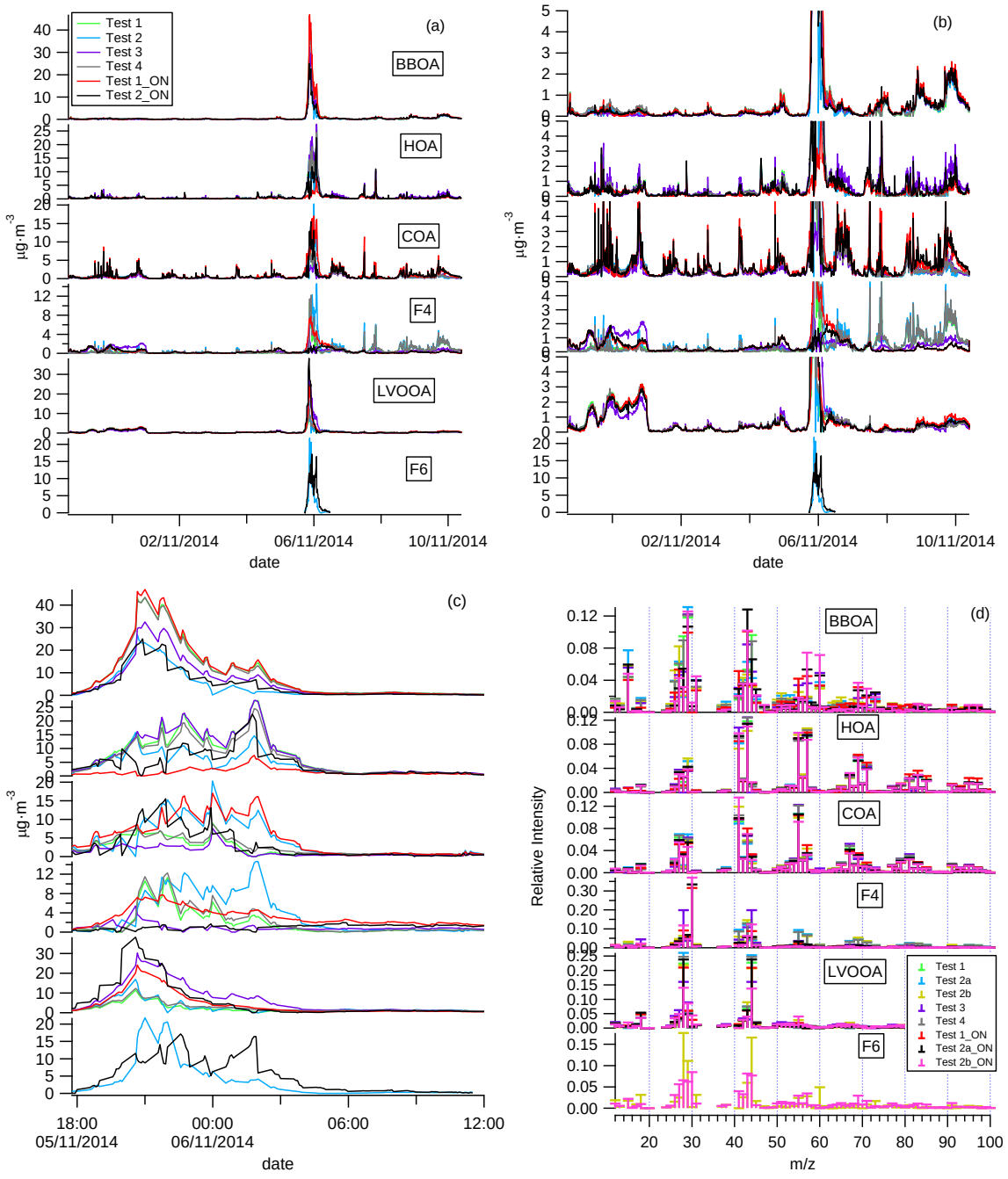

Figure S7: Comparison of the chosen solution for the four tests performed. Time series for the complete dataset (a), time series with a close up to y-axis to show low concentrations (b), time series during bonfire night period (c) and mass spectra.

S6.3 Comparison of different solution tests.

Here, the different tests performed without modifying the fragmentation table (test 1, test 2, test 3, and test4) modifying it (test1_ON and test2_ON) are compared in order to determine the test that better separates OA factors.

The analysis was carried out by comparing the residuals and Q/Qexp for m/z's and time series for all the dataset (figure S8) and more into detail for the bonfire night (figure S9); trilinear regression between BBOA, HOA and COA with NOx (figure S10) and diurnal profiles (figure S11).

Analysis without modifying the fragmentation table was the first experiment performed, where test 2 resulted to be the test that better deconvolved OA factors with; low residuals (figures S8 and S9) and low chi square, used as a goodness of fit (figure S10). Then test1_ON and test2_ON were performed in order to determine the best way to deconvolve OA sources including organic nitrate factors, where test 2 showed to be a better way to deconvolve OA sources compared to test1_ON.

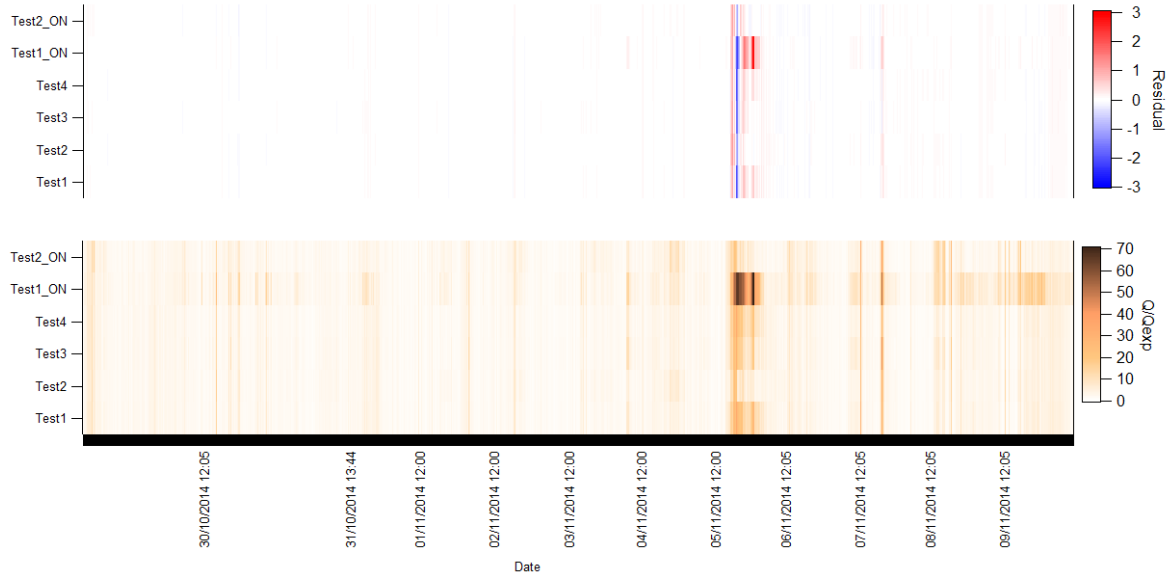

Figure S8: Comparison of the different solutions for all sampling period.

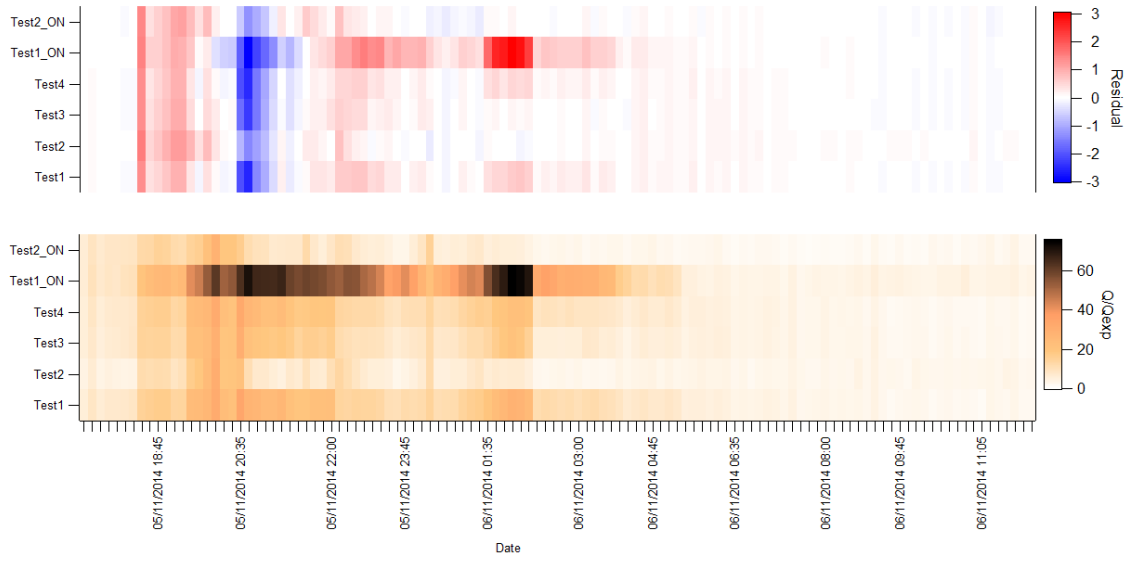

Figure S9: Comparison of the different solutions for the bfo sampling period.

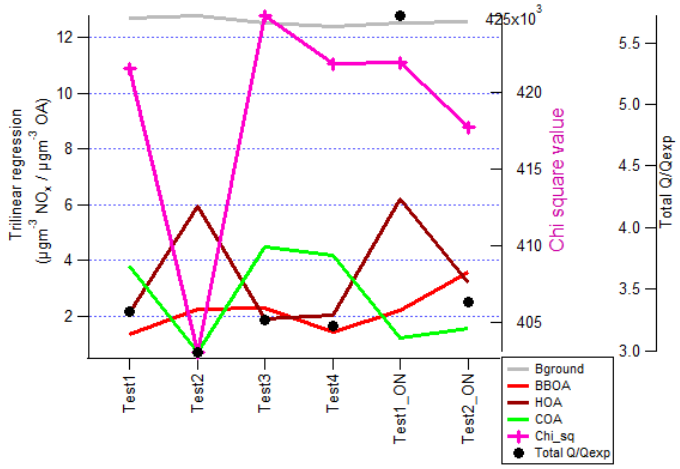

Figure S10: Trilinear regression between OA sources and NOx.

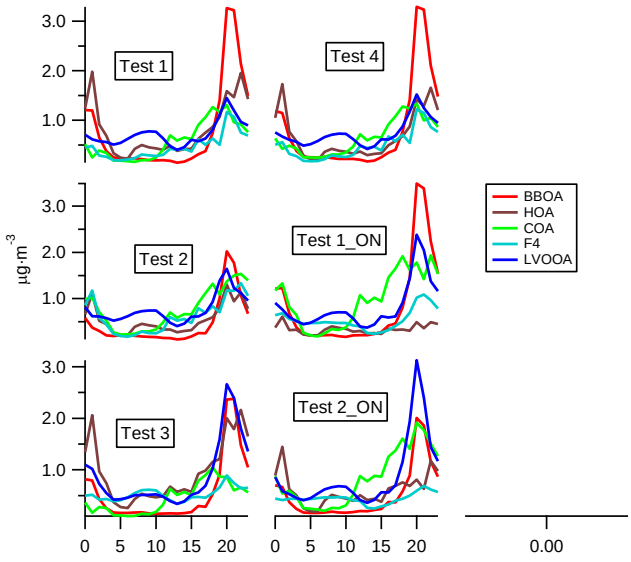

Figure S11: Diurnal profiles.

S7. Primary (pPON) and secondary (sPON) organic nitrate estimation.

The slope from a linear regression between PON, obtained from 46:30 ratios analysis in Section S5, and BBOA was used to calculate primary and secondary organic nitrate. Blue circles show the period where the slope between PON and BBOA was calculated (Section 4.2 in main text).

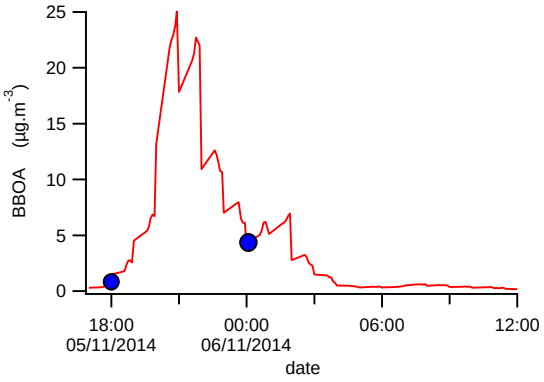

Figure S12: Time series used to calculate the slope between PON and BBOA

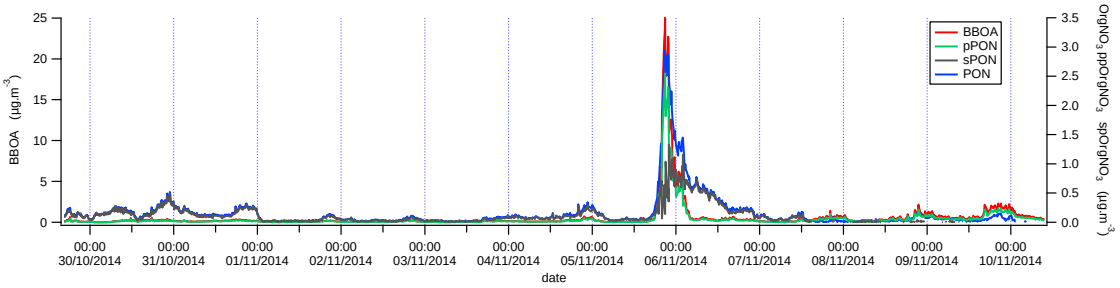

Figure S13: Time series of pPON and sPON for the whole period.

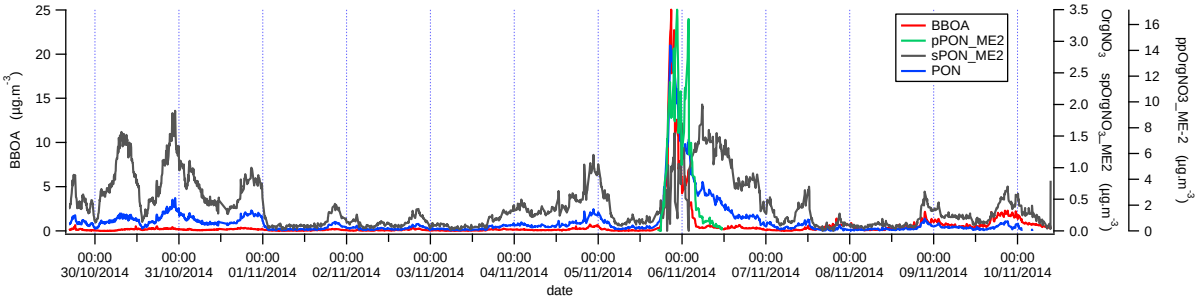

Figure S14: Primary (pPON_ME-2) and secondary (sPON_ME-2) organic nitrate time series obtained from ME-2 analysis.

S8. R2 values between OA sources and CIMS measurements.

Tables S3 show the r^2 values between the OA factors and CIMS measurements, for the different analyses; ALL, LC, bfo and WL. Only R^2 higher or equal to 0.6 are displayed.

Table S3: R^2 values between OA factors and CIMS measurements.

		BBOA				COA	LVOOA				sPON		pPON
Formula	Name	ALL	LC	bfo	WL	bfo	ALL	LC	bfo	WL	LC	WL	bfo
C3H7NO2	L-Alanine			0.81		0.73			0.64				0.67
* CO		0.79		0.81	0.67	0.80							0.78
HONO	nitrous acid	0.73		0.72	0.65	0.60	0.72		0.81				
C6H6O3		0.76	0.72	0.71	0.82		0.77	0.64	0.82			0.61	
C2H5N3O2				0.71					0.88				
C5H7Cl				0.70			0.73		0.87				
C7H6O2	Benzoic acid	0.76		0.70	0.80		0.79		0.82			0.62	
C2H4IO3	Glycolic acid			0.70					0.72				
C2H5NO	Methylformamide	0.71		0.64			0.72		0.73				
* NO				0.63									
* SO_2				0.63									0.72
* NO_x				0.60									
CHN	Hydrogen cyanide	0.69		0.60	0.66		0.68		0.66				
C5H10O2	Pentanoic acid	0.63		0.60			0.67		0.80				
C3H7NO	Propionamide	0.65					0.64		0.67				
C4H6O4	succinic acid								0.75	0.57			
C6H6O	Phenol	0.60					0.72		0.67				
C4H6O2	methacrylic acid	0.60					0.71		0.69				
C7H8O	Cresol	0.60					0.61						
C3H4O4	Malonic acid								0.63				
CHNO	Isocyanic acid						0.73		0.69				
H2O2										0.68			
C3H4O2	Acrylic acid						0.62		0.65				
C2H3NO	Methyl isocyanate						0.69		0.65				
C3H6O2	propionic acid				0.72		0.62					0.67	
ClNO3	Chlorine nitrate							0.66			0.60		
ClNO2	nitryl chloride							0.65					
C6H5NO3	nitrophenol									0.79			

ALL = all dataset, LC = low concentrations, bfo = bonfire night, WL = winter-like.

References

Arnott, W. P., Hamasha, K., Moosmuller, H., Sheridan, P. J., and Ogren, J. A.: Towards aerosol light-absorption measurements with a 7-wavelength aethalometer: Evaluation with a photoacoustic instrument and 3-wavelength nephelometer, Aerosol Science and Technology, 39, 17-29, 10.1080/027868290901972, 2005.

Coen, M. C., Weingartner, E., Apituley, A., Ceburnis, D., Fierz-Schmidhauser, R., Flentje, H., Henzing, J. S., Jennings, S. G., Moerman, M., Petzold, A., Schmid, O., and Baltensperger, U.: Minimizing light absorption measurement artifacts of the aethalometer: Evaluation of five correction algorithms, Atmos Meas Tech, 3, 457-474, 2010.

Crippa, M., DeCarlo, P. F., Slowik, J. G., Mohr, C., Heringa, M. F., Chirico, R., Poulain, L., Freutel, F., Sciare, J., Cozic, J., Di Marco, C. F., Elsasser, M., Nicolas, J. B., Marchand, N., Abidi, E., Wiedensohler, A., Drewnick, F., Schneider, J., Borrmann, S., Nemitz, E., Zimmermann, R., Jaffrezo, J. L., Prevot, A. S. H., and Baltensperger, U.: Wintertime aerosol chemical composition and source apportionment of the organic fraction in the metropolitan area of paris, Atmos Chem Phys, 13, 961-981, DOI 10.5194/acp-13-961-2013, 2013.

Farmer, D. K., Matsunaga, A., Docherty, K. S., Surratt, J. D., Seinfeld, J. H., Ziemann, P. J., and Jimenez, J. L.: Response of an aerosol mass spectrometer to organonitrates and organosulfates and implications for atmospheric chemistry, Proceedings of the National Academy of Sciences of the United States of America, 107, 6670-6675, 10.1073/pnas.0912340107, 2010.
Ji, D., Li, L., Pang, B., Xue, P., Wang, L., Wu, Y., Zhang, H., and Wang, Y.: Characterization of black carbon in an urban-rural fringe area of beijing, Environmental Pollution, 223, 524-534, https://doi.org/10.1016/j.envpol.2017.01.055, 2017.
Kiendler-Scharr, A., Mensah, A. A., Friese, E., Topping, D., Nemitz, E., Prevot, A. S. H., Äijälä, M., Allan, J., Canonaco, F., Canagaratna, M., Carbone, S., Crippa, M., Dall Osto, M., Day, D. A., De Carlo, P., Di Marco, C. F., Elbern, H., Eriksson, A., Freney, E., Hao, L., Herrmann, H., Hildebrandt, L., Hillamo, R., Jimenez, J. L., Laaksonen, A., McFiggans, G., Mohr, C., O'Dowd, C., Otjes, R., Ovadnevaite, J., Pandis, S. N., Poulain, L., Schlag, P., Sellegri, K., Swietlicki, E., Tiitta, P., Vermeulen, A., Wahner, A., Worsnop, D., and Wu, H. C.: Ubiquity of organic nitrates from nighttime chemistry in the european submicron aerosol, Geophys Res Lett, 43, 7735-7744, 10.1002/2016gl069239, 2016.
Kostenidou, E., Florou, K., Kaltsonoudis, C., Tsiflikiotou, M., Vratolis, S., Eleftheriadis, K., and Pandis, S. N.: Sources and chemical characterization of organic aerosol during the summer in the eastern mediterranean, Atmos. Chem. Phys., 15, 11355-11371, 10.5194/acp-15-11355-2015, 2015.
Reyes-Villegas, E., Green, D. C., Priestman, M., Canonaco, F., Coe, H., Prévôt, A. S. H., and Allan, J. D.: Organic aerosol source apportionment in london 2013 with me-2: Exploring the solution space with annual and seasonal analysis, Atmos. Chem. Phys., 16, 15545-15559, 10.5194/acp-16-15545-2016, 2016.
Sandradewi, J., Prevot, A. S. H., Weingartner, E., Schmidhauser, R., Gysel, M., and Baltensperger, U.: A study of wood burning and traffic aerosols in an alpine valley using a multi-wavelength aethalometer, Atmos Environ, 42, 101-112, 10.1016/j.atmosenv.2007.09.034, 2008.
Schmid, O., Artaxo, P., Arnott, W. P., Chand, D., Gatti, L. V., Frank, G. P., Hoffer, A., Schnaiter, M., and Andreae, M. O.: Spectral light absorption by ambient aerosols influenced by biomass burning in the amazon basin. I: Comparison and field calibration of absorption measurement techniques, Atmos. Chem. Phys., 6, 3443-3462, 10.5194/acp-6-3443-2006, 2006.
Sciare, J., d'Argouges, O., Sarda-Estève, R., Gaimoz, C., Dolgorouky, C., Bonnaire, N., Favez, O., Bonsang, B., and Gros, V.: Large contribution of water-insoluble secondary organic aerosols in the region of paris (france) during wintertime, Journal of Geophysical Research: Atmospheres, 116, n/a-n/a, 10.1029/2011jd015756, 2011.
Weingartner, E., Saathoff, H., Schnaiter, M., Streit, N., Bitnar, B., and Baltensperger, U.: Absorption of light by soot particles: Determination of the absorption coefficient by means of aethalometers, J Aerosol Sci, 34, 1445-1463, 10.1016/S0021-8502(03)00359-8, 2003.
Young, D. E., Allan, J. D., Williams, P. I., Green, D. C., Flynn, M. J., Harrison, R. M., Yin, J., Gallagher, M. W., and Coe, H.: Investigating the annual behaviour of submicron secondary inorganic and organic aerosols in london, Atmos. Chem. Phys., 15, 6351-6366, 10.5194/acp-15-6351-2015, 2015a.
Young, D. E., Allan, J. D., Williams, P. I., Green, D. C., Harrison, R. M., Yin, J., Flynn, M. J., Gallagher, M. W., and Coe, H.: Investigating a two-component model of solid fuel organic aerosol in london: Processes, pm1 contributions, and seasonality, Atmos Chem Phys, 15, 2429-2443, 10.5194/acp-15-2429-2015, 2015b.